

CERN LIBRARIES, GENEVA



CM-P00052557

PH I/COM-71/37
19 August 1971

Proposal to Study the Reactions

$\pi^+ + p \rightarrow \Sigma^+ + K^+$, $K^- + p \rightarrow \pi^- + \Sigma^+$ and other 2-Body
processes at 10 GeV/c

Å Eide, A Lundby, CERN

P J Carlson, E Johansson, Stockholm

V Gracco, S Ferroni, Genova

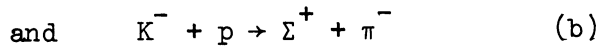
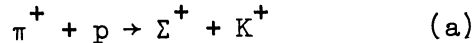
R J Homer, Birmingham University

C J S Damerell, B Ratcliff, T Tso, Rutherford Laboratory

August 1971

I GENERAL DISCUSSION

The hypercharge exchange line reversed reactions



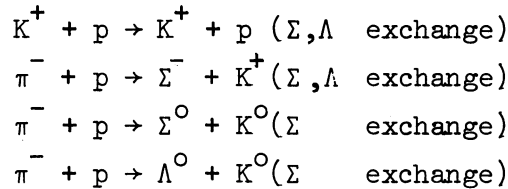
at high energy have so far been studied only over a very limited angular range. Fig 1 summarises the existing data in the region of 10 GeV/c, or at the highest available momentum when this is less than 10 GeV/c.

In contrast to these reactions, the elastic scattering and some inelastic channels (eg $\bar{p}p \rightarrow \pi^+ \pi^-$) have now been measured with good accuracy over most of the angular range. The difficulty with reactions (a) and (b) has not been, as one might at first think, the small magnitude of the cross-sections. In fact, these so far appear to be quite reasonable, consistent with the expectation for channels where both the forward and backward regions correspond to allowed Regge exchange in the t and u channels: see Fig 2. The problem rather lies in the very short decay length of the Σ^+ . Detection of the charged decay product (from $\Sigma^+ \rightarrow p\pi^0$ or from $\Sigma^+ \rightarrow n\pi^+$) is not difficult, but the tight constraints from the 2-body kinematics are lost. We are proposing an arrangement, largely using existing equipment, which is designed to tie down reactions (a) and (b) with rather complete angular coverage, and good background elimination. To be contrasted with Fig 1, we have in Fig 3 the sort of results which should come from the proposed experiment. The differential cross-sections are guessed, but the error bars indicate the expected quality of the data. In addition, the polarization of the Σ^+ should be obtained with an accuracy of a few percent over most of the angular range.

By measuring over a wide angular range, we should satisfy varied theoretical interests in the reactions. There has been evidence for some time that there may be a significant breakdown of line-reversal invariance for the hypercharge-exchange reactions in general, including reactions (a) and (b)⁵. However, there now appear to be some doubt about the data from reference (1) for reaction (a), and the cross-sections for the two reactions may in fact be converging with increasing energy.⁶

The region beyond $|t| \sim 1(\text{GeV}/c)^2$ has been explored only at 5 GeV/c incident momentum for reaction (a), and not at all for (b). One may expect structures which it will be of interest to compare with those already found in the elastic scattering at large angles.

Precise measurement of the backward peaks will be of interest. The backward region for reaction (b) should be compared with π^- -p elastic scattering (both Δ exchange, which is anomalously low for the π^- -p backward scattering). The backward region for reaction (a) contains contributions from both Σ and Λ exchange, and the data must be discussed in conjunction with existing measurements of backward peaks in



For kinematic reasons, we restrict ourselves to the decay mode $\Sigma^+ \rightarrow p + \pi^0$. This has the advantage that we automatically measure the Σ^+ polarisation. This polarisation is already known to be substantial in the forward region (out to $|t| \sim 2(\text{GeV}/c)^2$), and rather independent of energy. It will be particularly interesting to make the measurement in the backward peak region (and, for example, to compare with the measurements for backward π^- -p elastic scattering).

As regards competition from other experiments, there is a proposal⁷ to measure all helicity amplitudes for reactions (a) and (b) in the Ω spectrometer. The proposal covers only the forward region, and will be subject to systematic uncertainties in the measurement of the differential cross-section (because of the polarised target material). It is therefore complementary to our proposed experiment, rather than in competition with it.

II BEAM AND HYDROGEN TARGET

Because of the very small cross-sections beyond $|t| \sim 0.3(\text{GeV}/c)^2$ it is essential to work with the highest beam intensity obtainable from the accelerator. If the experiment is run in the D30 beam, the flux of K^- becomes inadequate above about 10 GeV/c.

The possibility has been discussed of building a high momentum beam of much higher intensity in the West Hall. Such a beam would be particularly useful for our proposed experiment. It would enable us to make a more precise measurement of $K^- + p \rightarrow \Sigma^+ + \pi^-$ at 10 GeV/c, and later allow the possibility of studying the energy dependence at higher momenta.

As in the present running, (Experiment S91) the use of a high intensity beam is made possible by excluding active spark chamber planes from the beam both before and after scattering.

Although we would operate with a rather wide momentum acceptance ($\pm 1\%$ for the positive beam and $\pm 3\%$ for the negative beam), hodoscope counters would be used to define the momentum of each incoming particle to $\pm 0.3\%$. The position of the incoming trajectory through the hydrogen target would be defined to $\pm 1.5\text{mm}$ in X and Y, and the incident direction to $\pm 0.5\text{ mrad}$.

Based on typical PS operating conditions, the incident pion flux in the positive beam is then 3.5×10^5 particles/pulse out of a total of 2.2×10^6 particles/pulse. The corresponding figures for the negative beam are 5.7×10^5 particles/pulse (total) and $9.9 \times 10^3 K^-$ /pulse.

A series of threshold Cerenkov counters along the beam line will be used to identify all particles (p, K^+, π^+ or \bar{p}, K^-, π^-) incident on the target. After traversing a final beam counter B1, the beam passes through the liquid hydrogen target T of length 100 cm.

III GEOMETRY 1 (FORWARD SCATTERING)

For both reactions, it is essential to make an accurate missing-mass measurement by determining precisely the momentum and direction of the forward particle. In conflict with this requirement is the need for good angular and solid angle acceptance. A suitable compromise is the geometry shown in Fig 4. We plan to use two spectrometer magnets each running at about 15 KGauss. M_1 is a spectrometer magnet from the Rutherford Laboratory (type M_5) and M_2 would be either a pair of CERN C Magnets or a CERN H magnet. Both magnets would be run with a vertical aperture of 50cm. The magnets would be run for most of the time in the polarity indicated (bending the beam and the wanted particles to the left). However we would pick up the region of very small $|t|$ by running for a short period with the magnet polarities reversed.

C_1 is a pressurized Cerenkov counter filled with Freon 13 B1. Such a counter (of size rather smaller than is needed here) has already been constructed by us.

C_2 is an atmospheric pressure Cerenkov counter used to tag scattered pions.

The trigger will consist of the appropriate beam logic (Cerenkov counters flagging π^+ or K^-); with B_V in anti-coincidence to exclude the residual beam; signals from the counter arrays T_R and T_L ; and the appropriate signals from C_1 and C_2 ($\check{C}_{K+\pi} \cdot \check{C}_\pi$ for reaction (a); $\check{C}_\pi \cdot \check{C}_\pi$ for reaction (b)). Because the direction of the proton from Σ decay follows closely the Σ direction, except for very small $|t|$, we shall be able to restrict the allowed combinations of elements from T_L and T_R to a coincidence matrix. This procedure, which is normally followed for studies of 2 body processes, is valuable for the removal of background events, which tend to have forward going particles in each arm of the detection system.

There will be other veto counters around the region of the target to eliminate inelastic events with several charged secondaries.

$W_1 - W_6$ are capacity read-out wire spark chambers with 0.5 mm wire spacing, used to make a precise momentum measurement on the forward scattered particle. These will give nearly a factor 2 improvement in the spatial resolution relative to the chambers currently in use, which have 1.0 mm wire spacing.

Chambers W_7 to W_{10} are used to measure the direction of the proton from the decay of Σ^+ . It will sometimes (though not usually) be possible to see evidence of the finite path traversed by the Σ before decay.

Even with C_2 in the logic, the trigger rate will initially be rather high, because of the large flux of forward particles. Dead time losses are minimised by the short recovery time (~ 5 msec) of the spark chamber system. In addition, the very small cross-section in the large $|t|$ region means that one can quickly turn off the hodoscope counters closest to the beam.

DATA RATES

Fig 5(a) shows the solid angle acceptance as a function of t , with the small $|t|$ region shown in detail in Fig 5(b). The calculation includes a reasonable cut on the momentum of the decay proton, which causes some loss of events in the very forward region. In order to fully utilize the geometrical acceptance it is necessary that the Cerenkov counters should have good efficiency over a horizontal angular range of 16° for C_1 , and 20° for C_2 .

Putting in these acceptances, the beam intensities already mentioned, and a factor 0.5 for the fact that we are interested only in the decay mode $\Sigma^+ \rightarrow p\pi^0$, we obtain the following data accumulation rates

| | | |
|--------------|------|------------------------|
| Reaction (a) | 1600 | Events/ μ barn/day |
| Reaction (b) | 50 | Events/ μ barn/day |

Assuming $0.01 \mu\text{b}/(\text{GeV}/c)^2$ to be the minimum cross-section we shall have to measure, and assuming binning in t intervals of $2 (\text{GeV}/c)^2$ for the wide angle region, we obtain at least the following quantities of data in each angular bin.

| | | |
|--------------|-----|--------------------------------------|
| Reaction (a) | 350 | Events in 10 days with positive beam |
| Reaction (b) | 20 | Events in 17 days with negative beam |

We have made rather pessimistic assumptions about the background level in the analysis in assigning the guessed errors in Fig 3.

BACKGROUND

Reaction (a) Given no identification of the forward particle, one could

measure the missing mass assuming it to be a kaon. The region of Σ missing mass would then be dominated by events from inelastically scattered (but high momentum) forward pions, with a substantial background from forward protons.

From the experience of the Michigan - Argonne group at 5 GeV/c, we know that the inclusion of C_2 in the logic (C_π) is sufficient to show signs of the Σ missing mass peak (Fig 6(a)). The background can be substantially reduced by demanding a particle in the Σ decay cone. There is little point in measuring the momentum of this particle, because of the large range allowed by the decay kinematics. In addition, there is not much to be gained by making a Cerenkov identification of this particle as a proton. The encouraging feature of the 5 GeV/c data is that the background is falling as fast as the signal over the t range covered (see Fig 6(b)-(e)).

At 10 GeV/c the background is likely to be relatively worse because of the reduced cross-section for reaction (a). For this reason we propose to eliminate forward protons in the experiment by the use of C_1 . Then the missing mass spectrum, apart from the effect of Cerenkov inefficiency, should reflect the true distribution for events associated with a K^+ in the final state. Indeed, the Michigan - ANL group have taken data at 5 GeV/c with such a combination of Cerenkov counters. The resultant extremely clean distribution of missing mass is shown in Fig 6(f). Apart from $\pi^+p \rightarrow \Sigma^+K^+$, the main contribution comes from $\pi^+p \rightarrow \Sigma^+(1385) + K^+$.

The missing mass resolution which can be achieved in our setup will be similar to that in Fig 6(f). The momentum resolution on the incident beam (standard deviation) of 0.3%, the angular resolution on the incident beam of 0.5 mrad, the momentum resolution on the forward scattered particle of $\leq 0.5\%$, and the angular resolution of 1.0 mrad (including effects of multiple scattering), leads to a resolution on the missing-mass squared of $\sim 0.10 (\text{GeV})^2$ (standard deviation). The calculated missing-mass resolution vs t is plotted in Fig 9. This is clearly adequate provided that no unexpected phenomenon (such as copious production of low-mass $\Lambda\pi$) sets in at wide angles.

IV GEOMETRY 2 (BACKWARD SCATTERING)

So far, the backward scattering region for reactions (a) and (b) has not been explored other than with bubble chambers. The design of an experiment to cover this region is consequently more speculative than for the forward scattering.

The proposal layout is shown in Fig. 7. We have left the proton-detecting arm unchanged from Geometry 1, except for the inclusion of C_2 now in the forward region to be used as a pion veto.

To cover a wide t range in the backward region, we would run most of the time in the polarity bending to the right. As for the forward geometry, the end of the angular range would be covered by reversing the magnet polarity.

C_1 would be run at higher pressure (and have thicker windows) than in Geometry 1, in order to flag π s down to 1 GeV/c. Ks in the angular range concerned would be below threshold for this counter.

Backward of 90° in the lab, we continue the Cerenkov counter system with a counter C_3 containing liquid nitrogen. This counter will be an improved version of the simple one which operated successfully in a recent experiment at ANL⁹. Kaons of up to 1 GeV/c are easily distinguished from pions.

In addition, a time-of-flight measurement to the array T_R will improve the kaon identification up to about 700 MeV/c.

The trigger logic for this geometry is essentially as for geometry 1, with C_1 , C_2 set to $\overline{C}_\pi \overline{C}_\pi$ (reaction (a)) and $\overline{C}_\pi \overline{C}_\pi$ (reaction (b)). It will be noticed that, in contrast to Geometry 1, we have not eliminated the contribution from protons to the missing mass distribution. However, this will not be a serious problem at the angles concerned, particularly since we have the pion veto on the left hand arm.

Chambers W1 - W5 are a selection of the $\frac{1}{2}$ mm wire spacing chambers from the right hand arm of Geometry 1. The arrangement shown in Fig 7 is conjectural. The actual arrangement will be a compromise between the conflicting requirements of maximum information content, - but minimum multiple scattering material.

Because of the large laboratory angles involved, the trigger rate will be low, and dead time losses will be negligible.

Because of the small angular range of the forward protons for this geometry, it would be possible to make a momentum measurement (using, for example, $\frac{1}{2}$ of M_2 from Geometry 1), with a rearrangement of the same chambers and counters, and with no loss of solid angle acceptance.

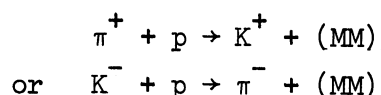
DATA RATES

The solid angle acceptance as a function of t is shown (for both M1 polarities) in Fig 8.

Since the acceptances are very similar to those for Geometry 1, we obtain similar rates of data accumulation (assessed as events/ μ barn/day). We would propose to run for the same time as with Geometry 1, and would then expect to obtain data in the backward hemisphere of quality indicated in Fig 3 (again, having made allowance for a rather large possible background in the missing mass distributions).

BACKGROUND

As described, the Cerenkov counters will provide a rather clean sample of events of the type



The question of background then reduces to the question of missing-mass resolution, in order to distinguish the events with Σ^+ produced. The resolution as a function of t (Fig 9) shows a more complicated variation than for Geometry 1. A major contribution comes from the uncertainty on the scattered K or π direction, due to multiple scattering in the target.

Nevertheless, the resolution is of good quality throughout the angular range.

V ABSOLUTE & RELATIVE NORMALIZATION

For both geometries, we are aiming for excellent absolute normalization (better than 5%) to allow accurate determination of differences between these

and other cross-sections. In any case, the cross-section differences between reactions (a) and (b) should be rather more accurate, because of having been measured in the same geometrical setup.

Nevertheless, this feature is far from sufficient to guarantee good relative normalization between these channels. The remaining difficulties are considerably more severe than those of a purely geometrical origin. We outline here the most important problems, and our intentions for handling them.

Firstly, there is the question of the incident beam profile. This will be different between the positive and negative beam, and will also be subject to time dependent variations (due to small misalignments of beam line elements, variation of magnet currents, variation in the internal beam of the P.S., etc). Problems of this type provided the major source of error in the Stony Brook experiment.¹ We would avoid such problems by the use of the beam hodoscope system, and by frequently taking runs triggering just on the beam logic, in order to have reliable beam profiles for input to the Monte Carlo acceptance calculation.

The efficiencies of the scintillation counters in the system will be periodically monitored. Barring accidents, these should be maintained at well over 99.5%, and should not give any trouble.

The spark chamber efficiencies for single tracks should be around 99%, and will be continuously monitored. In addition, the use of capacity read-out chambers (low spark energy) and decoupling between the chamber wires, should yield excellent multi-track efficiencies. We are constructing a system which will enable us to evaluate quantitatively the multi-track efficiency of the chambers under bench-test conditions¹⁰. The real problem with the spark chamber efficiencies comes at the stage of track reconstruction. It is difficult for programmes not to lose events in the presence of accidental tracks through the chambers. Such effects would be particularly serious because of the difference in intensity between the positive and negative beams. We propose to run some data at reduced intensity, and use this to assist in eliminating the final few percent inefficiency in the track reconstruction programmes for the data at normal intensity.

Finally (and most important) is the question of the efficiencies of the threshold Cerenkov counters C_1 , C_2 and C_3 . These have an immediate effect on the relative normalization between reactions (a) and (b), because they are used differently in the logic for the two channels. These counters will require careful design,

with calculation of the light transmission by Monte Carlo methods. From previous experience, it should be possible to achieve efficiencies in excess of 99% for wanted particles over the entire region of phase space required. The rejection of sub-threshold particles is determined by secondary processes such as δ -ray production. These effects will not give serious trouble in the present experiment. We intend to map the efficiencies of the counters over the entire phase space (which involves linear and angular scans in a test beam) before installing them in the experimental setup.

VI CHOICE OF INCIDENT MOMENTUM

From the preceding discussion, it appears that 10 GeV/c is about the maximum momentum at which reasonably complete angular coverage can be achieved. This momentum also provides a very useful second point for the energy dependence of the cross-section differences between reactions (a.) and (b) for small $|t|$. The first point is provided by bubble chamber experiments around 4 GeV/c, which seem to show reliably that at this momentum the K induced channel has a considerably larger cross-section than the π induced channel (\sim factor 2).

It would clearly be interesting (though of less direct significance) to know also the energy dependence for the large $|t|$ data. The backward cross-section should also be measured at another energy. To this end we would expect subsequently to propose a repetition of the experiment at lower energy.

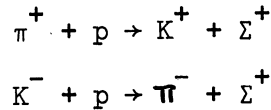
Nevertheless it appears desirable to run the 10 GeV/c data first, in view of the interest in the question of line reversal invariance for reactions (a) and (b) at high energy. Indeed, if the small $|t|$ data still shows cross-section differences at 10 GeV, the most important next step might be to go to higher momentum, concentrating just on the forward region.

VII DATA ANALYSIS

Apart from the on-line checking of the data, the bulk of the data analysis will be done outside CERN (probably at the Rutherford Laboratory). For data which is topologically reasonable, we shall make a fast, approximate missing mass calculation, and rapidly exclude events outside the region of interest. The number of events requiring the full fitting programme should be approximately equal to the number of good events in the experiment.

VIII SUMMARY

We propose to measure differential cross-sections and polarization for the line reversed reactions

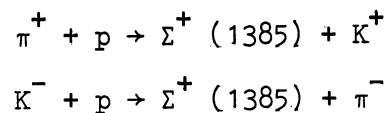


at 10 GeV/c, over most of the angular range. These measurements will be of good quality as regards absolute normalisation, and will allow accurate comparisons of the above cross-sections to be made, because the same setup will be used to study both reactions.

We request a total of 8 weeks of running time (to be split equally between the two geometries). In each geometry, we would run for $1\frac{1}{2}$ weeks with the positive beam, and $2\frac{1}{2}$ weeks with the negative beam. About 2 weeks of running time would be required for setting up the experiment.

In addition to the above reactions, we would obtain data on several other processes. Those which can most clearly be resolved will be the 2 body coplanar processes like πp and Kp elastic scattering, and $\bar{p} p \rightarrow X \bar{X}$ where $X = p, \pi, K$.

In addition, the improved missing-mass resolution relative to previous runs will allow the study of



with low background.

There is very little (or no) data on these channels at high momentum transfers.

The equipment involved on the experiment does not include anything particularly difficult, and much of it can be taken over from previous experiments.

In order to do the best possible experiment with the negative beam, we would strongly prefer to run in a high momentum zero degree beam from the Ω target in the West Hall.

ACKNOWLEDGEMENT

We wish to acknowledge helpful correspondence and conversations with Drasko Yovanovitch of ANL and Paul Grannis of Stony Brook, in connection with the design of this experiment.

REFERENCES

1. A Bashian, G Finocchiaro, M L Good, P D Grannis, O Guisan, J Kirz, Y Y Lee, R Pittman, G C Fisher and D D Reeder
1969 Stony Brook Conference Proceedings ("High Energy Collisions")
2. W A Cooper, W Manner, B Musgrave and L Voyvodic.
Phys Rev Letts 20, 472 (1968).
3. D Birnbaum, R M Edelstein, N C Hien, T J McMahon, J F Mucci, J S Russ, E W Anderson, E J Bleser, H R Blieden, G B Collins, D Garelick, J Menes and F Turkot, Carnegie-Mellon Preprint 1970.
4. Bubble Chamber data compiled by V Barger. Reviews of Modern Physics 40 138 (1968).
5. K Lai and J Louie, Nuclear Physics B19, 205 (1970).
6. C Quigg, Private Communication.
7. Proposal to EEC by CERN, Collège de France, Ecole Polytechnique and Orsay. PHI/COM-71/7.
8. D Yovanovitch, Private Communication.
9. H E Fisk (Carnegie-Mellon Group), Private Communication.
10. R Morgado, V Z Peterson, and L Shiraishi, Nucl Instr & Methods 94 189 (1971).

FIGURE CAPTIONS

- Fig 1 A) $\pi^+ + p \rightarrow K^+ + \Sigma^+$ Existing data around 10 GeV/c
 B) $K^- + p \rightarrow \pi^- + \Sigma^+$ Existing data around 10 GeV/c
- Fig 2 Regge exchange allowed in t and u channels for reactions
 (a) and (b)
- Fig 3 Fictitious data from proposed experiment for reactions
 (a) and (b). Error bars are believed realistic.
- Fig 4 Experimental setup for Geometry 1
 (Forward Scattering)
- Fig 5 Solid angle acceptance for Geometry 1
- Fig 6 Missing-mass plots for reaction (a) from reference 8.
- Fig 7 Experimental setup for Geometry 2
 (Backward scattering)
- Fig 8 Solid angle acceptance for Geometry 2
- Fig 9 Calculated missing-mass squared resolution (standard
 deviation) over full angular range

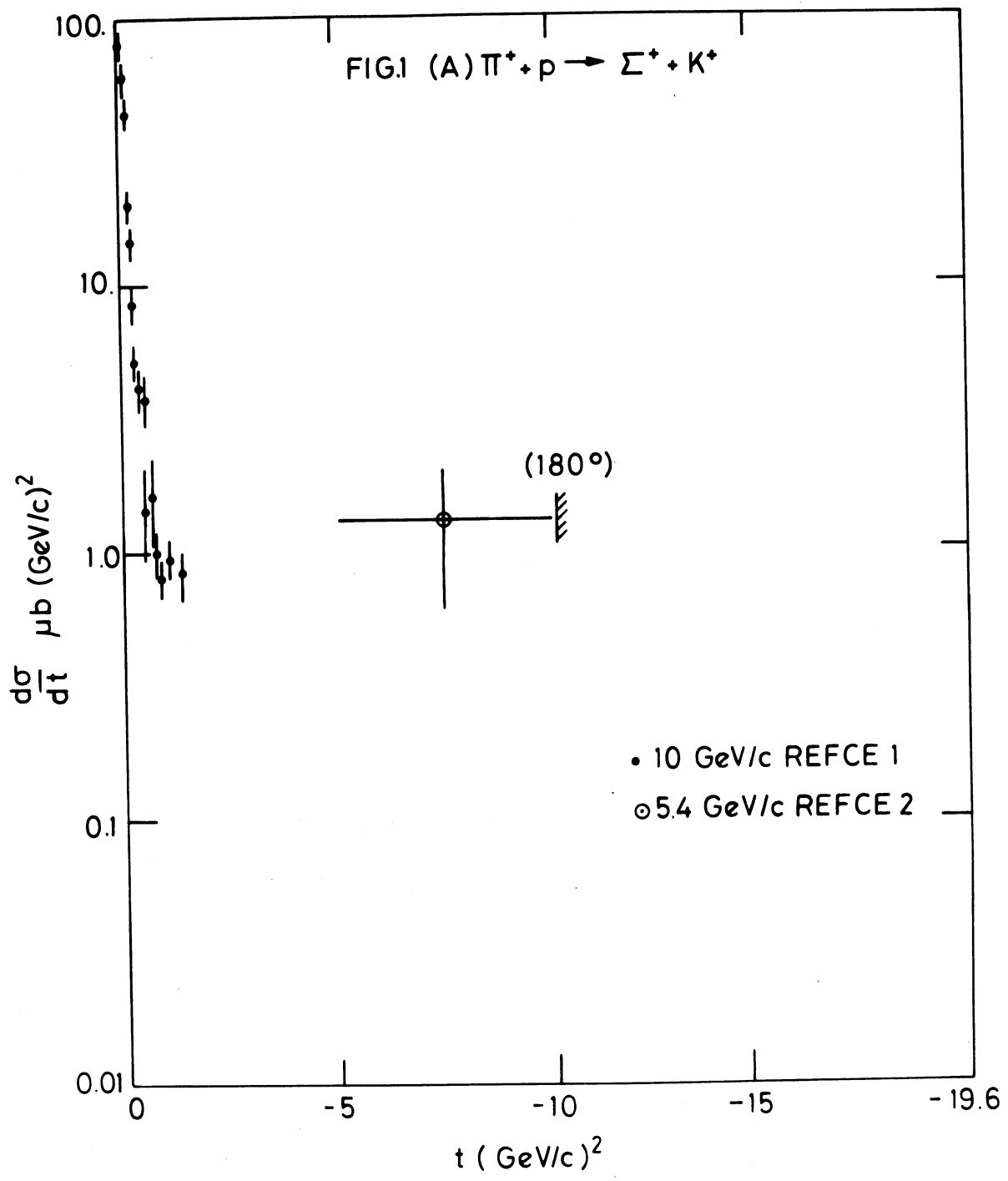
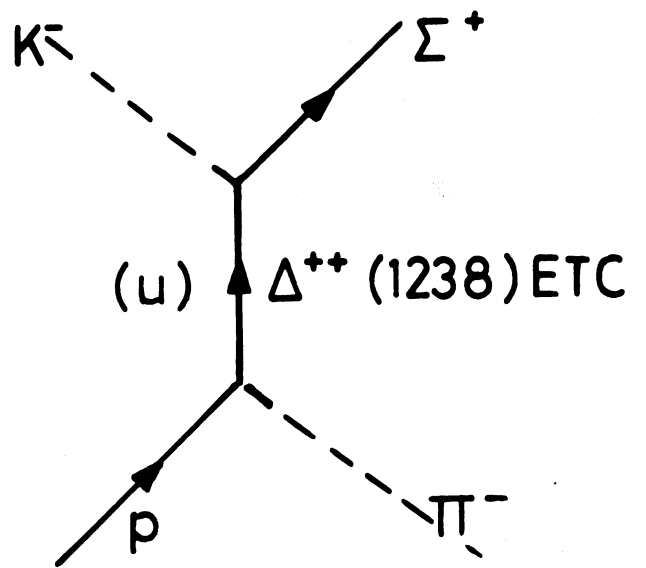
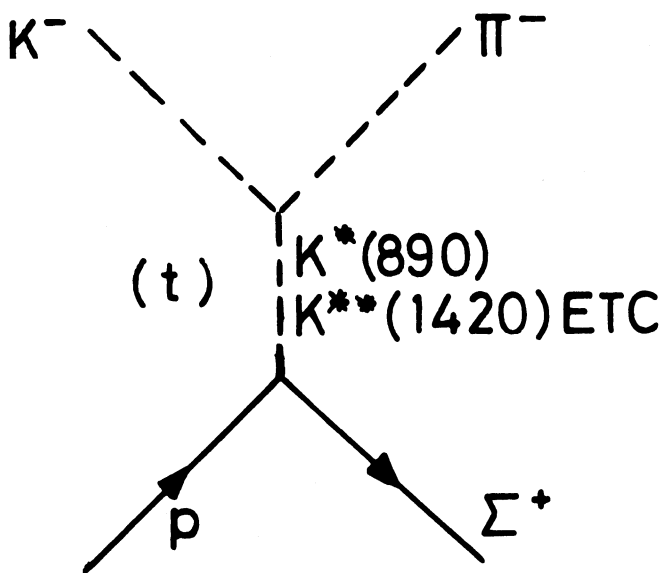
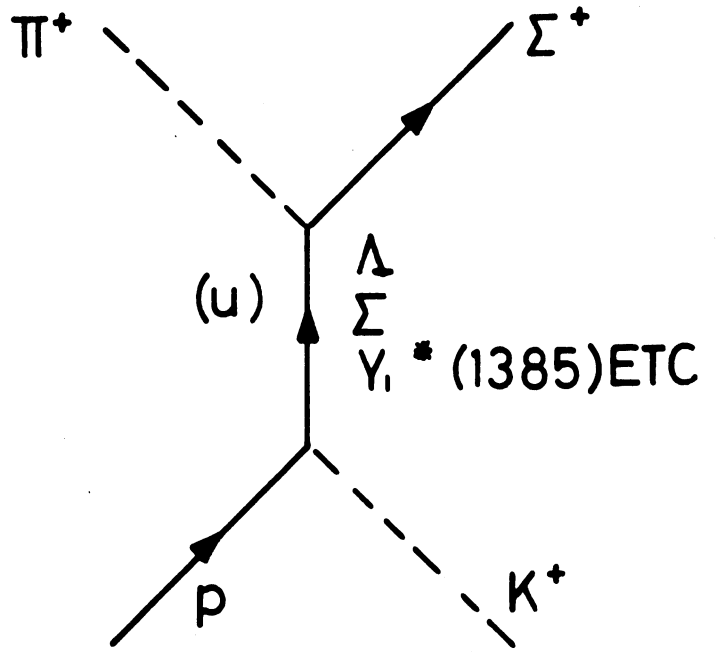
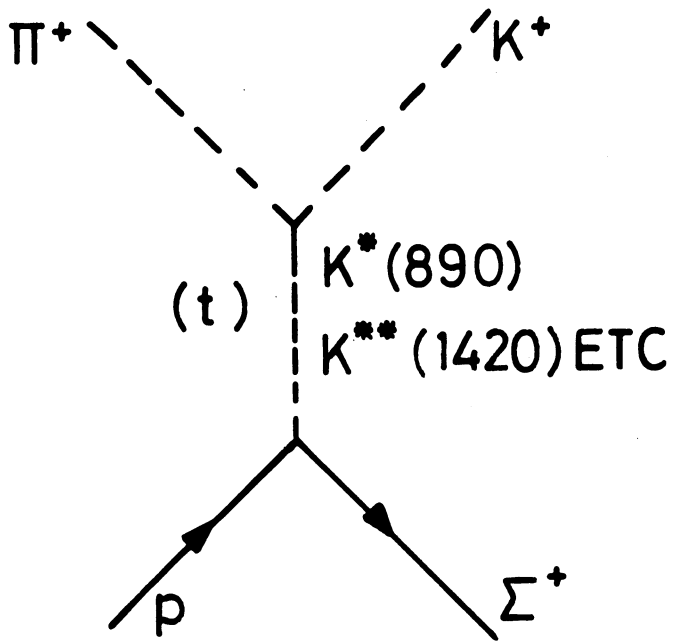
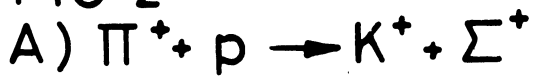
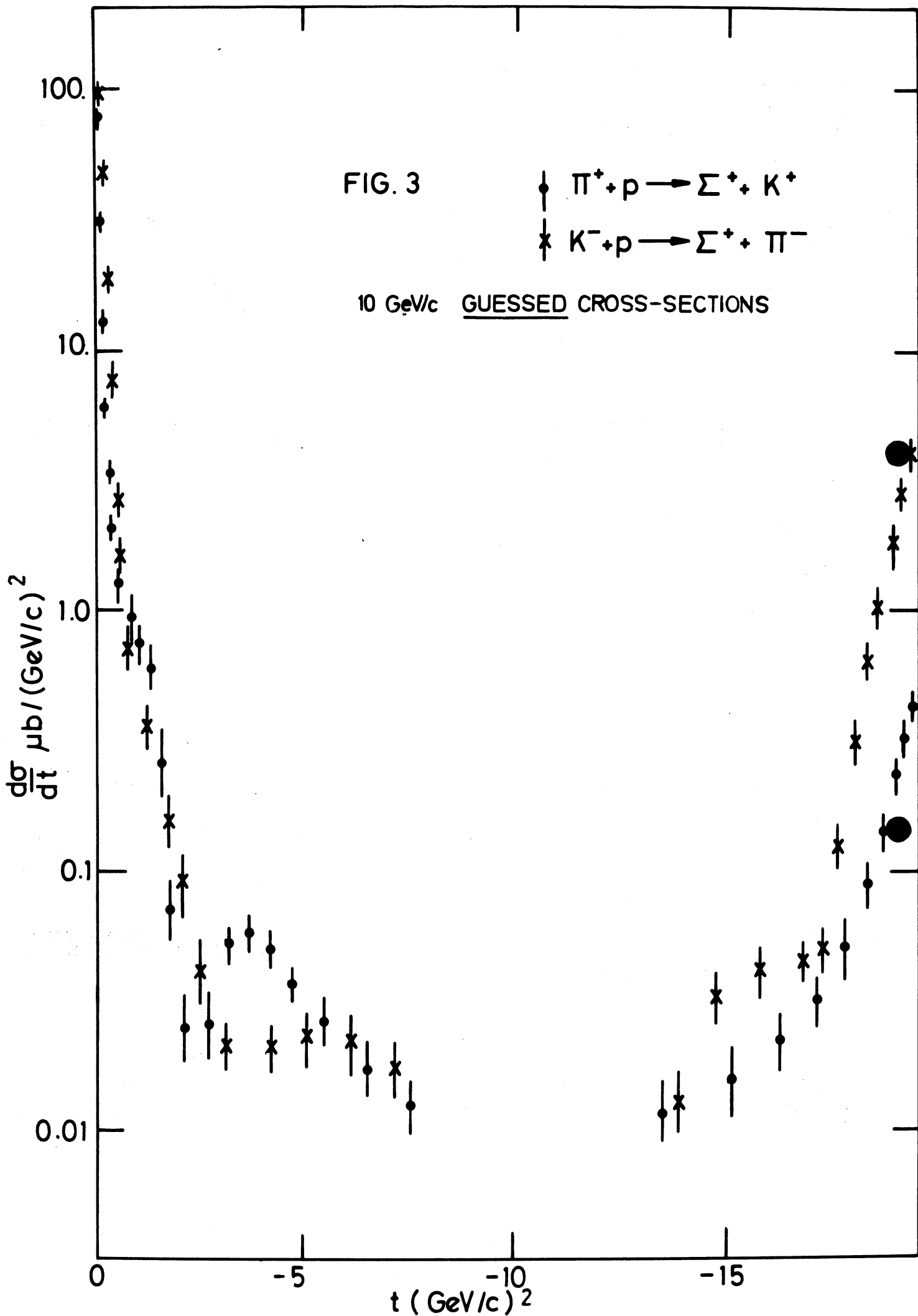


FIG 2





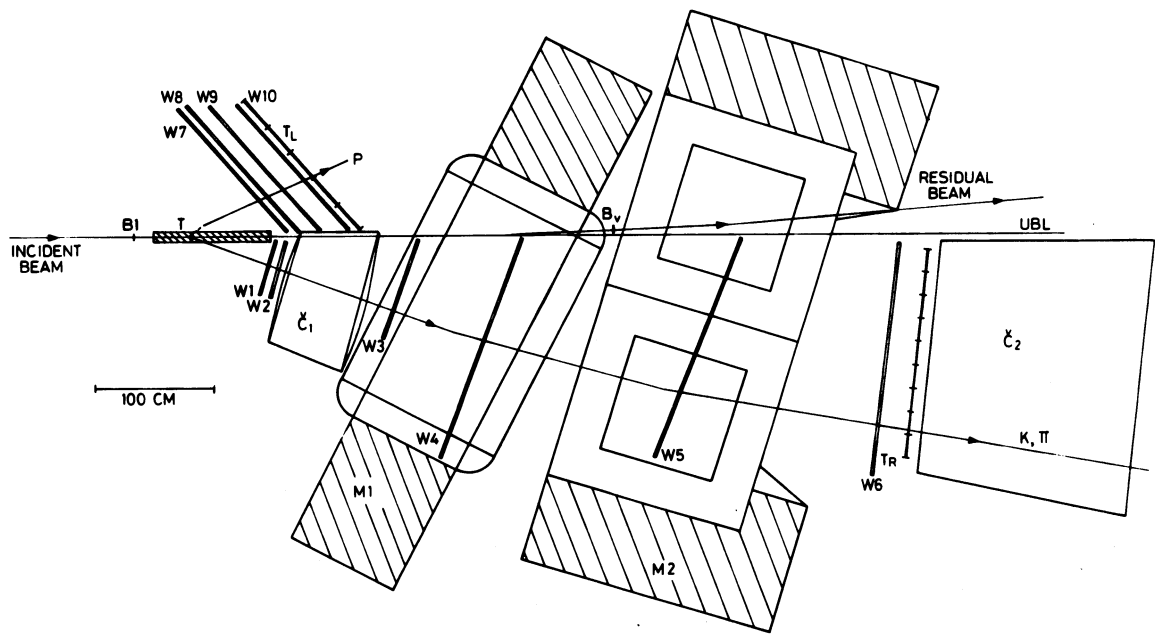
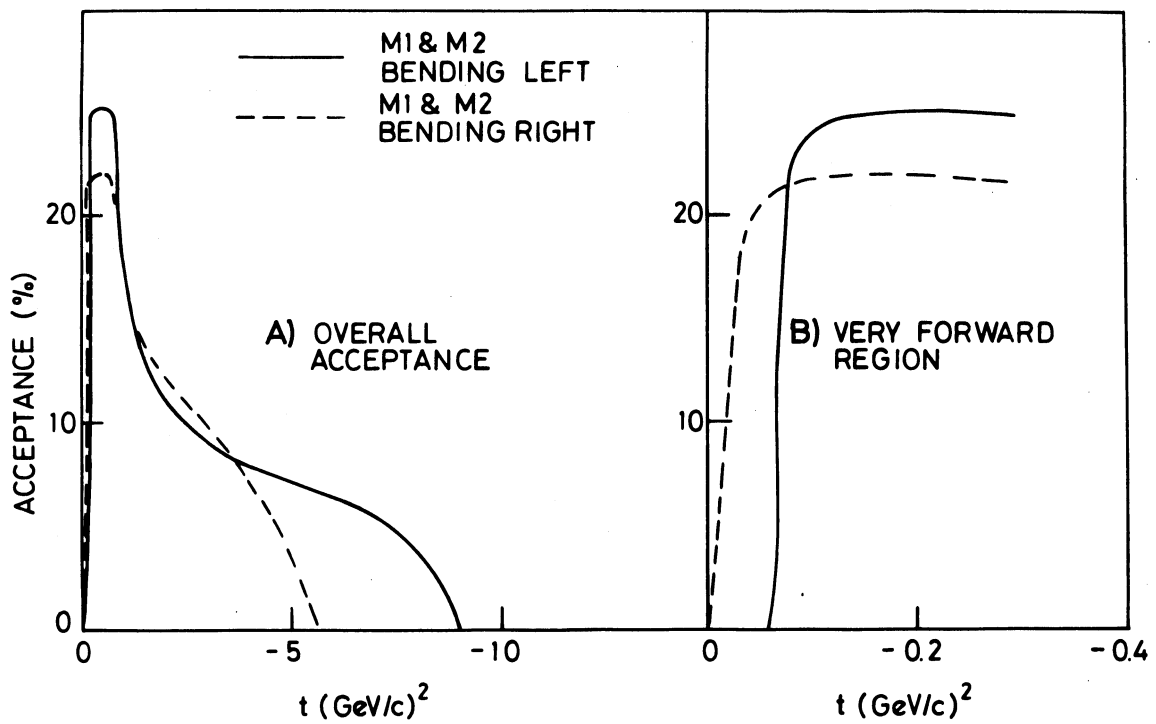
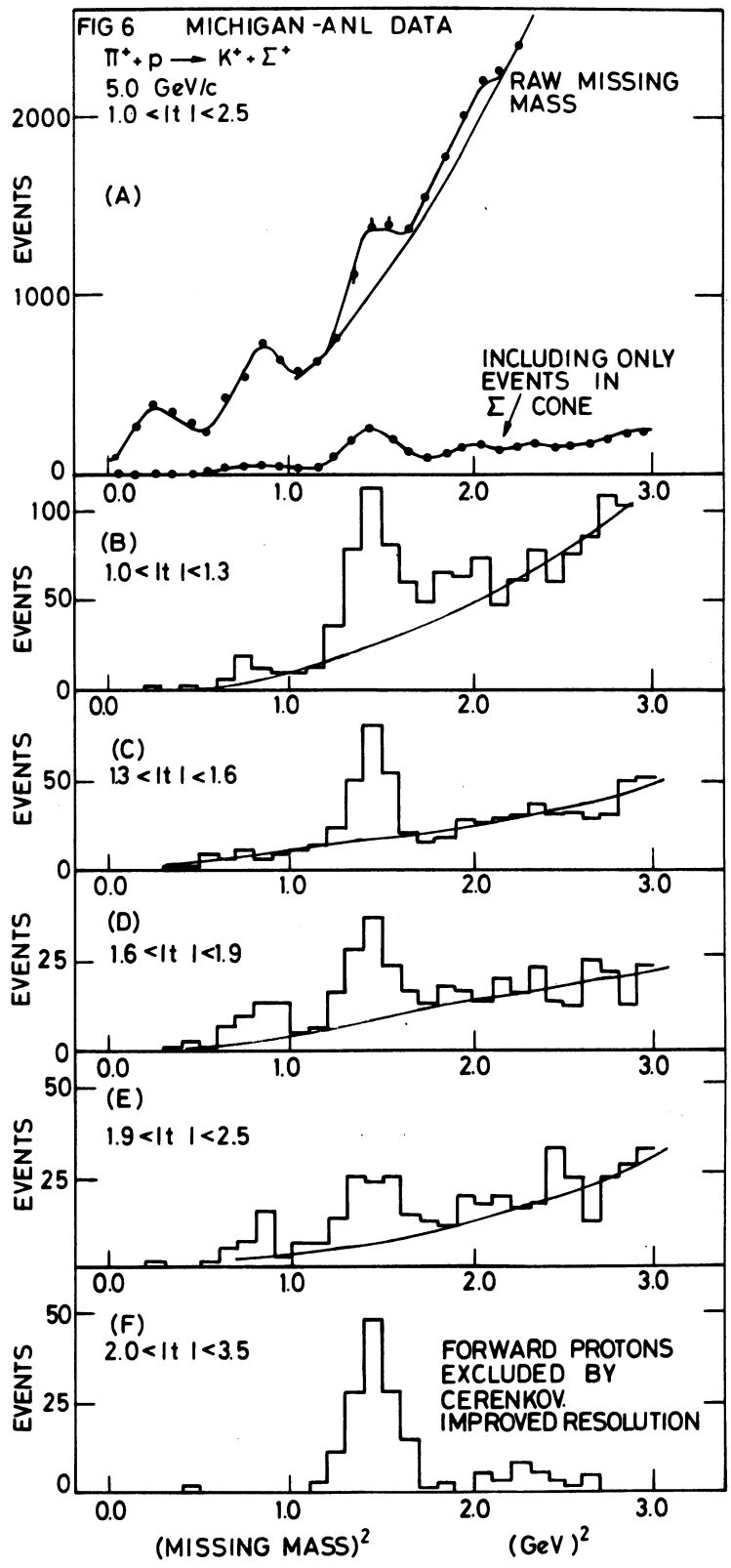


FIG. 4 GEOMETRY I (FORWARD SCATTERING)

FIG 5
10 GeV/c $\pi^+ p \rightarrow \Sigma^+ K^+$
ACCEPTANCE FOR GEOMETRY 1





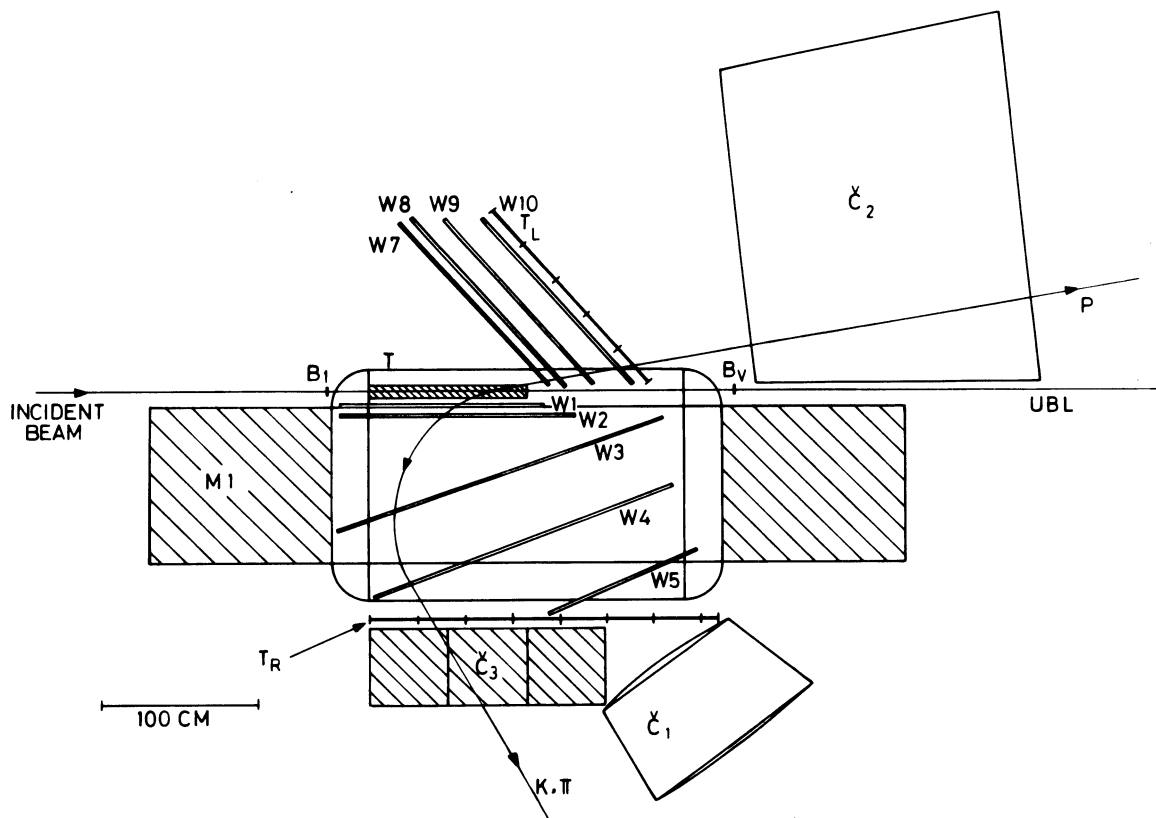


FIG. 7 GEOMETRY 2 (BACKWARD SCATTERING)

FIG 8. 10 GeV/c $\pi^+ + p \rightarrow \Sigma^+ + K^+$ ACCEPTANCE FOR GEOMETRY 2

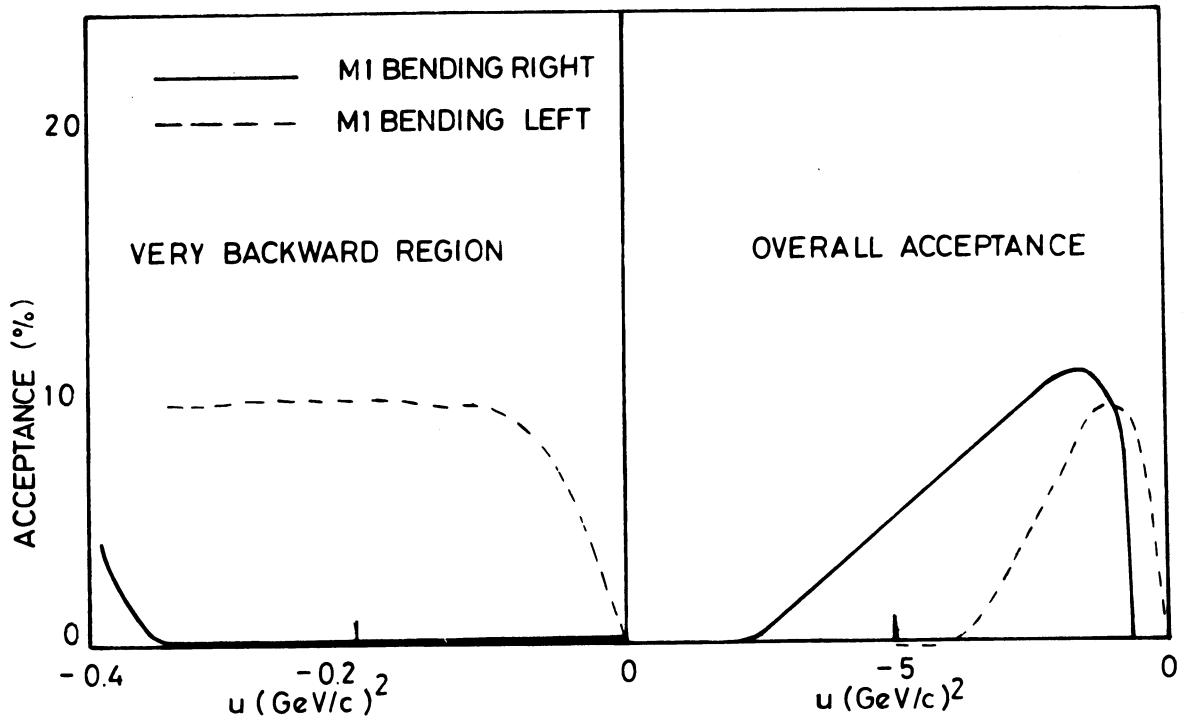


FIG 9. CALCULATED (MISSING MASS)² RESOLUTION

